

A numerical analysis on the performance of buckling restrained braces at fire-study of the gap filler effect

Elnaz Talebi^a, Mahmood Md. Tahir^{*},
Farshad Zahmatkesh^b and Ahmad B.H. Kueh^c

*Construction Research Centre, Faculty of Civil Engineering,
Universiti Teknologi Malaysia, 81310 UTM Johor Bahru, Malaysia*

(Received October 05, 2014, Revised February 04, 2015, Accepted February 08, 2015)

Abstract. Buckling Restrained Braces (BRB) have been widely used in the construction industry as they utilize the most desirable properties of both constituent materials, i.e., steel and concrete. They present excellent structural qualities such as high load bearing capacity, ductility, energy-absorption capability and good structural fire behaviour. The effects of size and type of filler material in the existed gap at the steel core-concrete interface as well as the element's cross sectional shape, on BRB's fire resistance capacity was investigated in this paper. A nonlinear sequentially-coupled thermal-stress three-dimensional model was presented and validated by experimental results. Variation of the samples was described by three groups containing, the steel cores with the same cross section areas and equal yield strength but different materials (metal and concrete) and sizes for the gap. Responses in terms of temperature distribution, critical temperature, heating elapsed time and contraction level of BRB element were examined. The study showed that the superior fire performance of BRB was obtained by altering the filler material in the gap from metal to concrete as well as by increasing the size of the gap. Also, cylindrical BRB performed better under fire conditions compared to the rectangular cross section.

Keywords: Buckling Restrained Braces (BRB); gap filler material; fire resistance; cross sectional shape; finite element analysis

1. Introduction

Bracing system is one of the most commonly used tools for enhancing the stiffness of structural frame in resisting lateral loads such as wind and earthquake. Due to the additional strength append to the structural frame by this system, it can also be used to sustain the compression forces, which are generated from fire loadings. In nonlinear deformation domain, ordinary bracing elements manifest low ductility and non-symmetrical hysteresis responses in tension and compression. Further deterioration of strength and degradation of stiffness in a bracing member are typically attributed to buckling under compression loadings. These shortcomings have drawn the attention

*Corresponding author, Professor, E-mail: mahmoodtahir@utm.my

^a Ph.D., E-mail: eln_tli@yahoo.com

^b Ph.D., E-mail: fa_zahmatkesh@yahoo.com

^c Ph.D., E-mail: kbahmad@utm.my

of structural engineers to explore and propose new bracing systems for better performance under various loading conditions. One of these promising systems is the Buckling Restrained Braces (BRB), which has been developed in recent decade owing to their excellent structural behaviour under axial loadings (Clark *et al.* 1999, Korzekwa and Tremblay 2009, López-Almansa *et al.* 2012, Nguyena *et al.* 2010, Sahoo and Chao 2010).

The principal strong specifications of these systems are high-energy dissipation capability, high ductility and almost symmetrical hysteretic responses in tension and compression. In terms of constituent components, BRBs are composed of a yielding steel core encased in a concrete-filled steel hollow casing to prevent its buckling (Fig. 1(a)), non-yielding and buckling-restrained transition parts as well as non-yielding and unrestrained end regions (Fig. 1(b)). About 60%-70% of the entire length of the core is restrained by the casing (Sahoo and Chao 2010). In these bracing systems, compression stresses are mainly sustained by the restrained portion of the core.

On the other hand, the yield strength of the steel core is much lower than that of steel tube casing. This allows the core to yield in the same manner during tension and compression prior to casing, thus enhancing considerably the energy dissipation capabilities of BRBs in comparison to the ordinary bracing systems. Due to the Poisson's effect on the steel core, it expands when it is compressed. To prevent the axial stress transition from the core to the restrainer (in-filled concrete steel tube casing), a certain amount of clearance between the core and concrete is provided to avoid friction between them (Fig. 1(c)). In addition to this gap, in order to minimize friction almost completely between the core and concrete, a de-bonding agent is applied also to the surface of the core, as shown in Fig. 1(a).

It is worth noting that buckling-restrained braces or any bracing system is used to resist somewhat rare and hazardous load case, such as winds and earthquakes. Hence, the potential of a simultaneous occurrence of these loads with sever fire condition is extremely low. Nevertheless, our concern in this paper focuses more on the issues of the generation of large axial forces within the structural members, and its consequences in terms of huge deformation due to fire loading only.

This type of bracing can be therefore acts multi-functionally for numerous loading situations stated above.

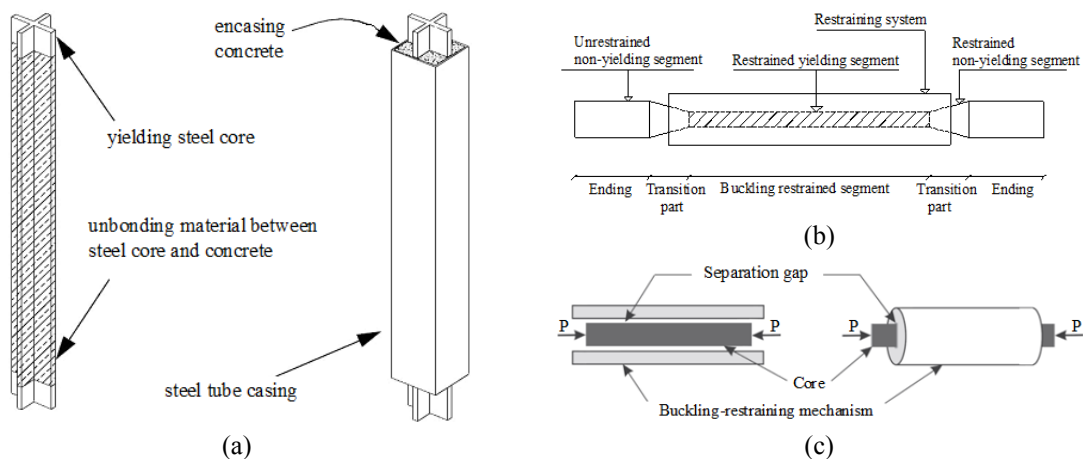


Fig. 1 Details of BRB as the (a) general structure (Clark *et al.* 1999); (b) steel core constituent segments; and (c) separation gap at steel core-restrainer interface (Korzekwa and Tremblay 2009)

The performance of BRBs under static and seismic loadings at ambient temperature has been well studied (Asgarian and Shokrgozar 2009, Mirtaheri *et al.* 2011, Takeuchi *et al.* 2010). The response of these systems at elevated temperatures has however been considered only in a limited number of literatures (Talebi *et al.* 2014a, b, Saitoh *et al.* 2005). Sahoo and Chao (2010) proposed a performance-based plastic design (PBPD) technique for designing the Buckling Restrained Braced Frame system (BRBFs). It was demonstrated that the BRBFs performed well in achieving acceptable yield strength as the storey drifts were computed to be within good expected range. López-Almansa *et al.* (2012) studied the cyclic behaviour of BRBs numerically using the finite element analysis that was validated by a series of experimental test results and analytical formulation proposed by them. They defined the behaviour of steel core using the damaged plasticity model. For in-filled concrete of steel tube casing, an isotropic damage property was prescribed. They showed that the stockier the steel core becomes, the lesser the transition of shear stress to the restrainer. Nguyen *et al.* (2010) compared three nonlinear static procedures, namely, modal, improved modal pushover analysis (MPA, IMPA) and mass proportional pushover (MPP) techniques in evaluating seismic performance of BRBs. Numerous modification factors, steel core lengths, fatigue properties and connections were studied in which the former two procedures offered better accuracy in assessing the allowable storey drifts in the structural frames. Takeuchi *et al.* (2010) investigated the effect of local buckling as it affected the strength and ductility of BRBs, with particular attention to the critical restraint condition of the steel core. Also, in order to verify the restrainer's buckling influence on the overall strength and stiffness of BRBs, different shapes of steel tube casing with varying wall thicknesses were analyzed numerically and experimentally. They showed that the thinning of the restrainer's wall thickness and the enlargement of gap at steel core-restrainer interface contributed to the increase in the strain at the restrainer wall. Furthermore, it was found that variation of core length did not affect considerably the local buckling behaviour. Mirtaheri *et al.* (2011) concluded that the length of steel core significantly affects the overall response of BRBs due to its direct influence on the energy dissipation of bracing element. Asgarian and Shokrgozar (2009) investigated the influence of structure's height and various arrangements of bracing elements on the response modification factor of BRB system. They suggested the values of 8.35 and 12 for the corresponding factors in order to achieve the ultimate and allowable stress limit states, respectively. In relation to temperature change responses, Talebi *et al.* (2014a) studied numerically how an individual BRB element performed with circular cross-section under standard fire condition. They declared that elevated temperature behaviour of BRB element was found to be similar to that of room temperature, i.e., the steel core yielded prior to the restraining system. The failure of bracing element was determined as a result of both reduction in material strength and increase in compression stress, due to temperature rise under fire condition. They proposed that limited temperatures for the linear behaviour of steel casing and in-filled concrete under standard fire are 196°C and 3°C, respectively. Saitoh *et al.* (2005) conducted an experiment to study the behaviour of BRBs in presence of an axial load during standard fire. They deployed steel mortar planks as restrainer for various cross section areas. They showed that when the outer surface of the mortar plank is coated with isolated materials, BRBs perform exceptionally well under fire condition.

Nowadays, the use of BRB systems has been expanded worldwide due to their superior structural performance. Considering the fact that the thermal conductivity of steel material is relatively high and its strength and stiffness descend dramatically at elevated temperatures (Zahmatkesh and Talebi 2010, Zahmatkesh *et al.* 2014), it is of paramount importance to study the thermal behaviour of steel and its composite elements in BRBs under any probable fire loading. In

this work, a three-dimensional nonlinear finite element model was developed to investigate the behaviour of BRBs during standard fire. The nonlinear finite element analysis package, ABAQUS version 6.9 (2008), was utilized to perform the thermal and structural analyses. The accuracy of proposed numerical model was first validated with the experimental test results recorded by Saitoh *et al.* (2005). Following validation, the thermal responses of BRBs, including the temperature-time histories in different locations of the brace were studied. The structural responses, such as axial contraction level of the specimens due to fire loading were also subsequently examined. Finally, a brief conclusion based on the main findings is provided.

To appreciate the nature of present research work better, a brief discussion on the existing relevant experimental test (Saitoh *et al.* 2005) is provided below.

2. Summary of the existing fire tests on BRBs

The particular experiment referenced here (Saitoh *et al.* 2005) was carried out at the Hamamatsu NICHIAS Corporation Laboratory, where the sample was mounted in an upright position, with the lower part fixed firmly while the upper part was pin supported. Four samples were provided and about 800 mm of the top and bottom ends of the specimens were wrapped with a refractory coating such that only 1250 mm of the remaining length was under a direct heat. Experimental evaluation of the sample's fire-resistance capacity was based on the operational procedure standards given by the International Building Code (ICC 2009). Performance of structure was evaluated for one-hour heating time. The allowable axial force proportionate to 441 kN (cross section area \times F/1.5) was prescribed in the axial direction of the steel core and heating was initiated to conform an average internal temperature of the furnace, θ , according to the formula given in Eq. (1).

$$T = 345 \log_{10} (8t + 1) + 20 \quad (1)$$

Where t is the heating elapsed time in minutes. Finally, at the end of the test, temperature-time histories at different locations of BRBs section along with the maximum axial contraction levels of the specimens were determined. It is noteworthy to mention that during the tests, Saitoh *et al.* (2005) considered different amount of moisture content within the samples.

3. Numerical FE model

3.1 Problem description

Various types and sizes of gap filler materials and their influence over the performance of BRB system in cases of fire was investigated. In terms of cross sectional shape effect, the suitability of each BRB section on resisting fire was also examined through three samples, namely, T1, T2 and T3. Each of these samples comprised of C-channel type of steel tube and the gap in the core's strong axis was filled with various materials. The BRB element schemas and cross sections of the samples are depicted in Fig. 2. The gap in sample T1 was filled with 10 \emptyset round steel bar, while the filler material of sample T2 was replaced by concrete. The gap in sample T3 was filled with thicker concrete (Fig. 2(b)). To have a benchmark on comparing the response of samples with each other, sample T1 was assumed as the standard sample. We took into account the same

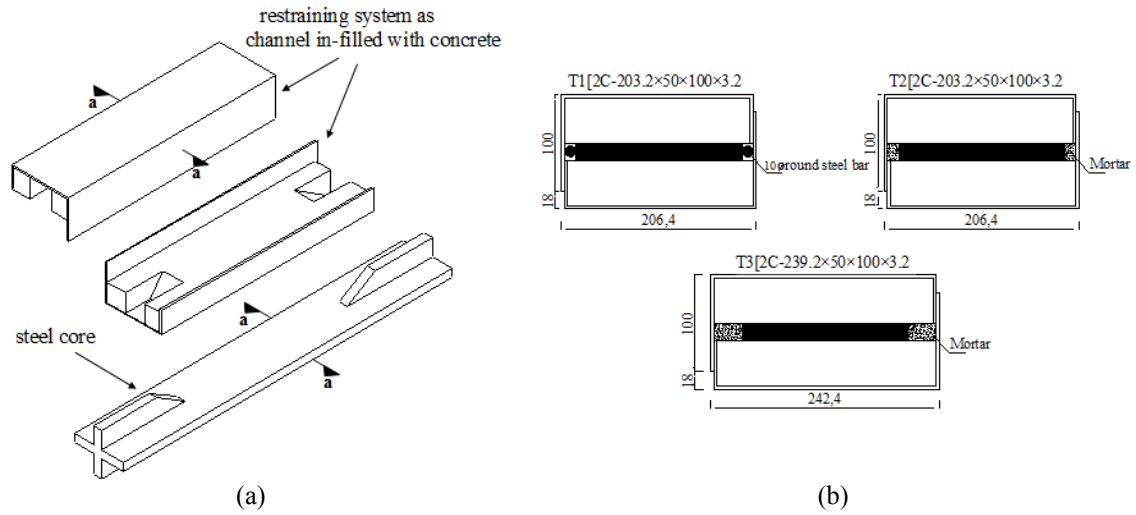


Fig. 2 (a) BRB elements and (b) a-a cross section of samples

specifications and settings adopted by Saitoh *et al.* (2005), such that we could have a conforming comparison with their experiment.

The cross-sectional area of each brace core in the models was equal to 2816 mm² with a yield and tension strength of 287.9 N/mm² and 441.8 N/mm², respectively. The steel core and steel casing conformed with standardized sections of PL-176×16 (SN400B) and PL-3.2 (SS400), respectively. The detailed description of samples specifications is provided in Table 1.

Table 1 Samples description

Sample	Core material Dimension (mm)	Cover C-channel dimension (mm)	Filler material
T1	176 × 16	2[203.2 × 50 × 100 × 3.2]	10Ø round steel bar
T2	176 × 16	2[203.2 × 50 × 100 × 3.2]	concrete
T3	176 × 16	2[239.2 × 50 × 100 × 3.2]	concrete

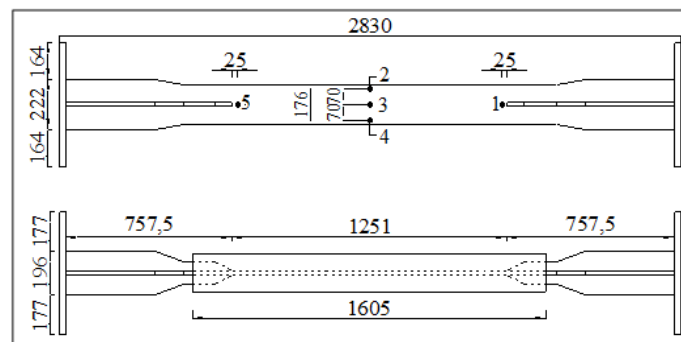


Fig. 3 Positions of the specified points for determining the temperatures in various locations of core at fire

Since the temperatures within the furnace and the steel casing in BRBs are expected to be slightly different during fire, the temperature of the sample was measured at 5 specified points on the steel core in the proposed numerical model (points 1-5 in Fig. 3).

3.2 Material properties

Two types of material properties for concrete and steel were deemed necessary in the study, namely, thermal and mechanical. The temperature-dependent thermal properties of steel recommended in Eurocode 3 (EC3 2005) were adopted. The thermal properties of concrete at elevated temperature followed those of Eurocode 4 (EC4 2005). The moisture content of concrete was taken into account via a maximum value of specific heat, which indicated the latent heat of water vaporization. According to EC4 (2005), this maximum value is 2020 J/kg K for a moisture content of 3% of the concrete weight, and 5600 J/kg K for a moisture content of 10%. The recommended value of moisture content of 3% was adopted for the siliceous aggregates in concrete. In the ABAQUS program, a classic metal material model was selected for the steel non-linearity, which followed the Von Mises yield function and associated plastic flow rule (Sun *et al.* 2012). Steel temperature-dependent mechanical properties as displayed in Fig. 4(a) were adopted as recommended in EC3 (2005).

The maximum compressive strength of concrete at the normal temperature (20°C), f_c , was prescribed as 30 N/mm² and the corresponding strain, ϵ_c , was taken as 0.0025. Fig. 4(b) shows the reduction factors that were applied on the concrete strength at elevated temperatures according to EC4 (2005), where T20 denotes the strength of concrete at normal temperature. A concrete damaged plasticity model (CDP) in ABAQUS was used for the fundamental relationship of concrete in the plastic domain. This model applies an isotropic damaged plasticity to demonstrate the nonlinear behaviour of concrete. It also contains the combination of non-associated multi-hardening plasticity and isotropic damaged elasticity to demonstrate the irreversible damage, which occurs through fracturing (Lu 2011).

Concrete exhibits multiple behaviours and damage mechanisms under compression and tension. Therefore, the stress-strain relationships of concrete need to be specified independently in tension and compression. The tensile characteristic of concrete at elevated temperature was defined as

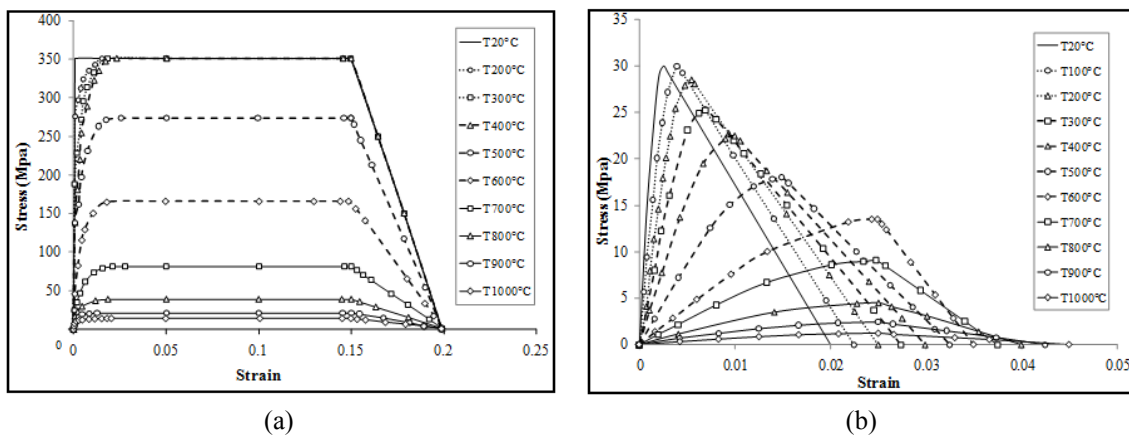


Fig. 4 Stress-strain relationship for the (a) steel and (b) concrete at elevated temperatures

the typical tensile stress-strain relationship that represented concrete damaged plasticity model as described in ABAQUS. The relevant values proposed by Jankowiak (2005) were adopted to model the damaged plasticity of concrete.

For the coefficient of thermal expansion (α), EC3 (2005) does not offer any provision. Hence, it can be computed as the first derivative of the equations proposed for the thermal strains of carbon steel, described in the following manner (Ho 2010)

$$\frac{\Delta L}{L} = 1.2 \times 10^{-5} T + 0.4 \times 10^{-8} T^2 - 2.41 \times 10^{-4}, \quad 20^\circ \text{C} \leq T < 750^\circ \text{C} \quad (2)$$

$$\frac{\Delta L}{L} = 1.1 \times 10^{-2}, \quad 750^\circ \text{C} \leq T \leq 860^\circ \text{C} \quad (3)$$

$$\frac{\Delta L}{L} = 2 \times 10^{-5} T - 6.2 \times 10^{-3}, \quad 860^\circ \text{C} < T \leq 1200^\circ \text{C} \quad (4)$$

Where T , ΔL , and L and denote the steel temperature, thermal elongation, and length of the element, respectively.

For the coefficient of thermal expansion of concrete, we adopted the same value that was proposed by Hong and Varma (2009).

3.3 Analysis procedure

In ABAQUS (2008), a sequentially-coupled thermal-stress analysis procedure was employed for the modelling. This technique was utilized since the stress-displacement solutions that are affiliated to the temperature history have no inverse dependency (ABAQUS 2008).

This approach consisted of two sequential analysis stages, where the outcome of the first step was used for the analysis in the second step. These steps are described as follows:

- (1) Heat transfer analysis was carried out to simulate the heat transfer inwards from the outer surface of the brace cross-sectionally, and along its length.
- (2) Stress analysis was carried out to simulate the structural response of BRBs exposed to fire or thermal loading resulted from step 1.

In order to transfer the thermal analysis results to the structural analysis correctly, the type of elements were constructed to be identical in both steps. Furthermore, the time steps in both procedures were consistently ensured such that the temperatures in thermal and structural analyses were compatible. Moreover, the consistency of the finite element meshes and node numbering were invoked in both steps to permit efficient response transmission.

3.4 Thermal analysis

The thermal reaction of element against heating is practically a transient heat transfer process, in which the heat from fire is transmitted to the outer surface of the brace by convection and radiation (Fig. 5(a)). It is then followed by means of conduction for the heat to navigate into the internal surfaces (i.e., steel tube, concrete casing and steel core), as shown in Fig. 5(b). Modelling of convective and radiative heat fluxes were considered as (Lu 2011)

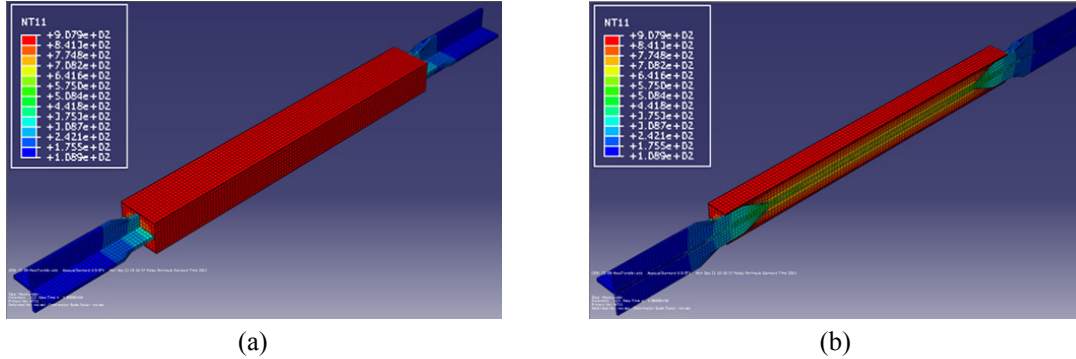


Fig. 5 (a) Outer surfaces of restrainer exposed to fire by convection and radiation; and (b) heat distribution from the heated surfaces of BRB to the inner surfaces by conduction within the longitudinal section (units for both legends are in °C)

$$q_{convection} = h_v(T_f - T_s) \quad (5)$$

$$q_{radiation} = \varepsilon_f \varepsilon_m \sigma \left[(T_f + T_0)^4 - (T_s + T_0)^4 \right] \quad (6)$$

Where q , h_v , T_f , T_s , T_0 , ε_f , ε_m and σ denote the heat flux, heat convective coefficient, temperature of fire, outer steel casing temperature, absolute zero temperature, emissivity of fire, emissivity of the steel surface and the Stefan-Boltzmann constant, respectively.

The fire loading was imposed uniformly along the whole length to the outer surface of steel casing (Fig. 5(a)) for a predefined heating time of one hour according to Equation 1, a temperature history proposed by the standard ISO 834 (1980). The cooling phase of fire was simulated according to the work done by Saitoh *et al.* (2005). For the standard fire exposure, the values of $h_v = 25$ (W/m²K), $\varepsilon_f = 0.8$ and $\varepsilon_m = 0.7$ as recommended by EC4 (2005) for composite elements were used. For idealization, we ignored simulating the end wrapping of BRB element as was implemented previously in the test.

In the thermal analysis, the model was meshed using three-dimensional eight-node solid elements (DC3D8) for the steel core, concrete and steel casing (restrainer). In spite of the existence of symmetry in cross section of the brace and fire furnace, a full brace was modelled. This is because previous study (Espinosa *et al.* 2011) has shown that in some instances the reaction of element is governed by the shear failure of concrete. Hence, unsymmetrical deformation is anticipated. In ABAQUS, the heating is initiated by means of increase in nodal temperatures. In terms of mesh density, 39688, 38548 and 39057 nodes, which amounted to 24952, 24274 and 24457 elements were defined for T1, T2 and T3 models, respectively. The results of nonlinear heat transfer analysis consisted of the temperature-time history for all nodes within the 3D model. They were subsequently applied as a thermal loading to the structural model.

3.4.1 Thermal contact at steel core-concrete and concrete-steel tube interfaces

Thermal resistance between the steel core-concrete and steel casing-in-filled concrete surfaces was modelled by applying a constant conductance coefficient of 200 W/m²K (Espinosa *et al.* 2011). The heat transfer radiation mechanism was ignored at the corresponding boundaries because of the limited clearance in the interfacial region to allow for a significant presence of air.

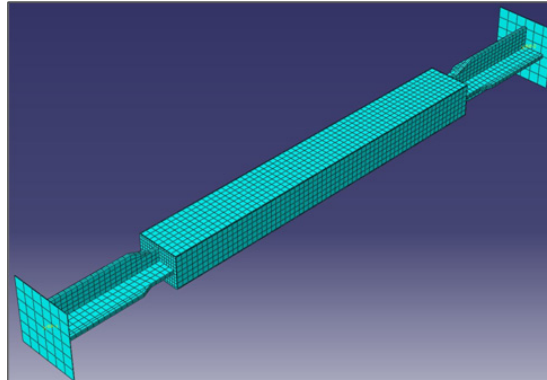


Fig. 6 3D finite element structural model for BRBs

3.5 Structural analysis

A nonlinear structural model was implemented after a full thermal analysis, taking into consideration the nodal temperature-time curves previously calculated from the thermal analysis. The three-dimensional eight-node solid elements with reduced integration (C3D8R) were used to mesh all parts of the bracing element (Fig. 6). Two steel endplates were added on to both endings of the core for implementing axial force and ending boundary condition of the brace. The endplates were modelled using the discrete rigid elements with all nodes coupled to a reference point located at the brace central axis at the ends. They were meshed using the four-node three-dimensional bilinear rigid quadrilateral elements (R3D4), in such a way that the total node numbers were then 40652, 39512 and 40174 as well as 25432, 24754 and 24875 elements for T1, T2 and T3 models, respectively. It was assumed that the top rigid plate could move along the brace axis but fixed in other transitional degrees of freedom. The bottom rigid plate was fixed in all transitional directions.

3.5.1 Mechanical contact at concrete-steel tube casing interface

The structural interplay between the casing and concrete surfaces were modelled as follows:

- (1) A node-to-surface formulation was defined for the contact description. “Hard contact” formulation was employed for the normal behaviour, in which pressure is transmitted between the surfaces only when they have contact with each other.
- (2) A Coulomb friction model was used to simulate the tangential behaviour of the contact pair.

When the bond strength is higher than the shear stress at the interface, no slippage between the surfaces takes place (Lu 2011). Conversely, when two contact surfaces experience relative slippage between them, a friction or shear stress is created. This shear stress is determined by the coefficient of friction and pressure in the interface. In this study, a constant coefficient of 0.3 was used since it had formerly generated accurate results for the contact between steel casing and in-filled concrete at room temperature simulation (Espinosa *et al.* 2011). The bond between the casing and the concrete was ignored, based on the consideration that the bond strength between the surfaces may be reduced rapidly at high temperatures.

3.5.2 Mechanical contact between concrete and steel core surfaces

Mechanical characteristics of contact between the steel core and concrete were the same as those mentioned in Section 3.5.1. The only difference was that a constant tangential friction factor equal to 0.1 was used for this interface. This is because in BRB system, a de-bonding material is applied on the surface of the core so that shear is not transferred to the restraining system. This value conforms to the friction factor for the steel and rubber.

4. Results and discussion

In cases of fire, it is expected that the exposed parts of BRB element, i.e., steel casing, non-restrained portion of the steel core and core stiffeners yield first due to their direct contact with fire. This can be seen from the results of FE modelling, which shows that the greater stresses were experienced by the steel core and its stiffeners (Fig. 7). Although the whole part of the casing was also exposed to fire and the expansion of tube was more than the restrained part of the core, it was evident that the steel casing had not experienced high stresses in the preliminary heating stages (Fig. 7). It is because in BRBs, the yield strength of steel casing is established to be much higher than that of steel core, in order to allow the restrained part of the core to yield first, under compression force. Hence, at elevated temperatures the steel core whose strength was lower than the other parts yielded first in presence of the applied axial force and the compression force that was generated within the brace due to fire loading. Consequently, the rate of yielding in the steel core was much higher than the expansion of casing. As a result, the behaviour of BRB at elevated temperature was analogous to that of normal temperature under compression force, i.e., the core yielded prior to the in-filled steel casing. This concept was discussed thoroughly in the previous work done by Talebi *et al.* (2014a).

For verification, the proposed numerical model responses were compared with the experimental observations recorded by Saitoh *et al.* (2005) for BRBs subjected to fire. The numerical thermal

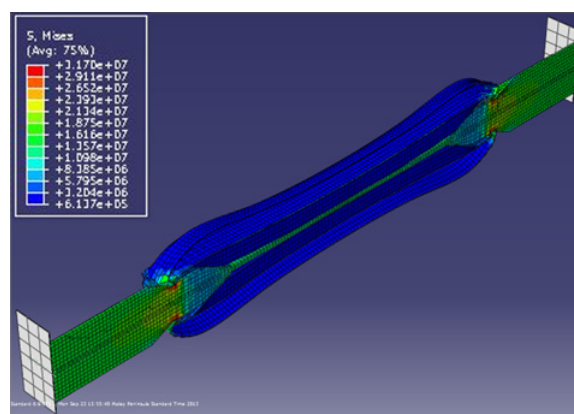


Fig. 7 Deformed shape of bracing element and the corresponding Von Mises stress (kg/m^2) within BRB, after exposed to fire

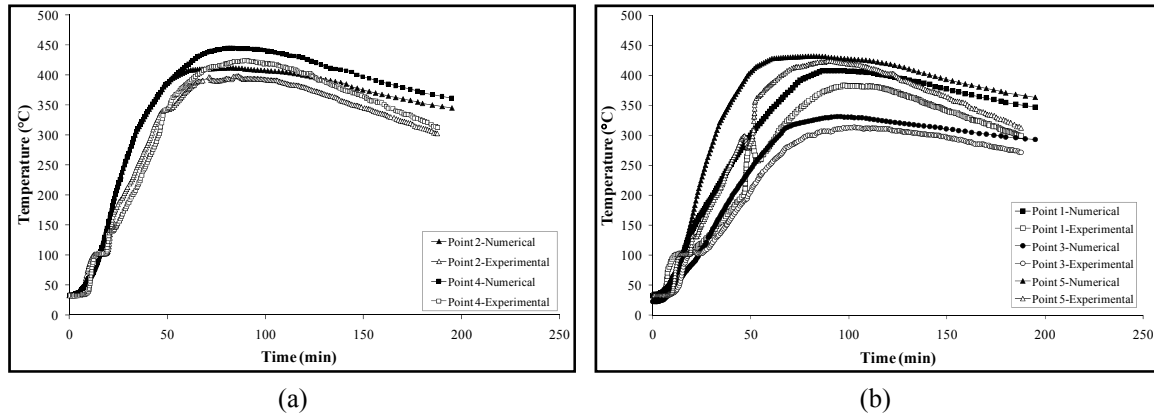


Fig. 8 Comparison of $T-t$ curves for BRB core section at (a) points 2 and 4; and (b) points 1, 3 and 5 in sample T1

analyses as well as experimental tests were performed for all BRB elements over a maximum period of 360 minutes of heating time.

The temperature-time responses ($T-t$ curves) of sample T1 at different locations of bracing core section (as specified in Fig. 3) were compared for numerical and experimental procedures in Fig. 8. Apparently, both approaches were in close agreement. Some discrepancies between the results were observed, such that the numerical method showed somewhat higher temperatures than that of the test. This could be because of the difference in the heating length of specimens considered for the proposed FE model and previous experiment.

4.1 Global observations

In order to investigate the response of each BRB sample during fire, it was assumed that specimens were exposed to heating for 1 hour and after that left alone for the application of purely axial force. In the numerical model, sample T1 was unable to sustain the specified axial force

Table 2 Temperature of steel core and elapsed time at specified points of each sample

Sample	Heating time	Maximum temperature at each point of the core (top values) and the corresponding time (bottom values)					Maximum temperature of the core at the elapsed heating time		
		1	2	3	4	5	43 min	48 min	51 min
T1	43	330 100	443 90	418 68	445 81	404 93	361	365	371
T2	48	352 115	439 102	437 105	440 100	365 103	314	320	327
T3	51	327 131	396 115	393 117	398 112	322 120	235	244	253

* Temperatures and times are in °C and minutes, respectively

(441 kN) and compression force that was developed within it during fire until the pre-determined 1 hour of heating time. Hence, in order to prepare a condition for the specimen to sustain the corresponding axial forces, the heating time was reduced in the analyses. Consequently, FE results showed that T1 could sustain the axial forces up to a temperature of about 361°C after 43 minutes of heating. The corresponding value in the experiment was 338.1°C after 47 minutes of heating. Detailed information on the maximum temperature at each specified point of the steel core and the elapsed heating time of corresponding temperatures within all specimens are provided in Table 2.

Fig. 8 shows that even after ceasing heating of T1 at 43 minutes in the FE thermal analysis, temperature of the core increased continuously. This is due to the existence of residual heat in the element, which reached the highest temperature of about 445°C after 81 minutes in the numerical analysis (Table 2). The comparative value in the experimental test was 419.2°C after 86 minutes, which was practically close to that modelled. In addition to a greater length of exposure to heating, which was followed by the superior residual heat in the FE model, the effect of meshing of brace in the finite element modelling can be attributed to the observed discrepancies.

4.2 Effect of the gap filler material at steel core-restrainer interface

To investigate the influence of altering the type of in-filled material of the gap on the fire resistance of steel core in BRBs, the effects of using concrete are shown in Fig. 9 for T2. By changing the type of gap filler material from steel to concrete, sample T2 was able to sustain the applied axial force and fire loading for about 5 minutes more than sample T1 with a temperature of about 320°C. In the comparative test, it was recorded as 297.3°C and the heating was terminated after 50 minutes. In a similar manner to T1, the latent heat in the steel core of T2 had also caused further rise in temperature reaching a peak value of about 440°C after 100 minutes (Table 2). The corresponding values from the experimental test were 416.4°C and 105 minutes, respectively. Despite of some observed discrepancies, there exist as a whole good agreements between the results of proposed numerical model and previously performed test.

Temperature distribution across the cross section and along the length of the heated brace for various in-filled materials of the gap from FE analyses are shown in Fig. 10. By focusing on the temperature range values, it can be seen that the temperature distribution from the heated surface

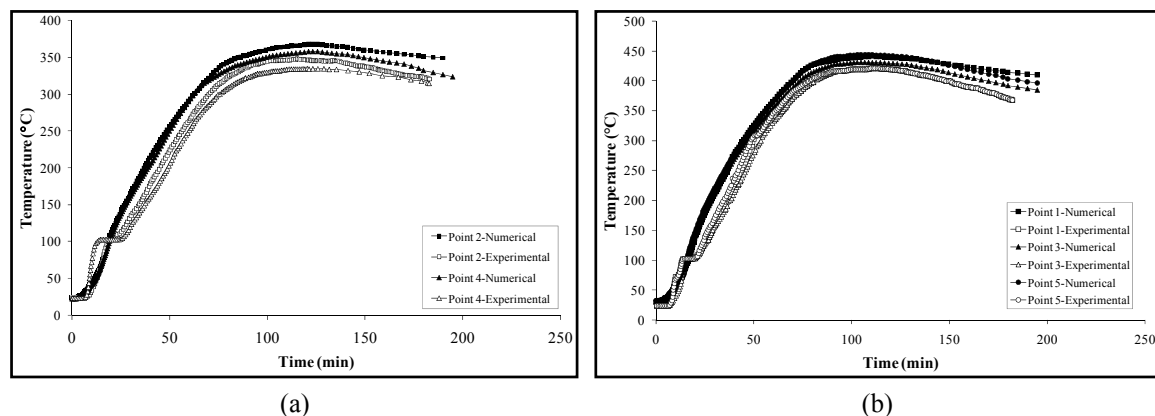


Fig. 9 Comparison of $T-t$ curves for BRB core section at (a) points 2 and 4 and (b) points 1, 3 and 5 in sample T2

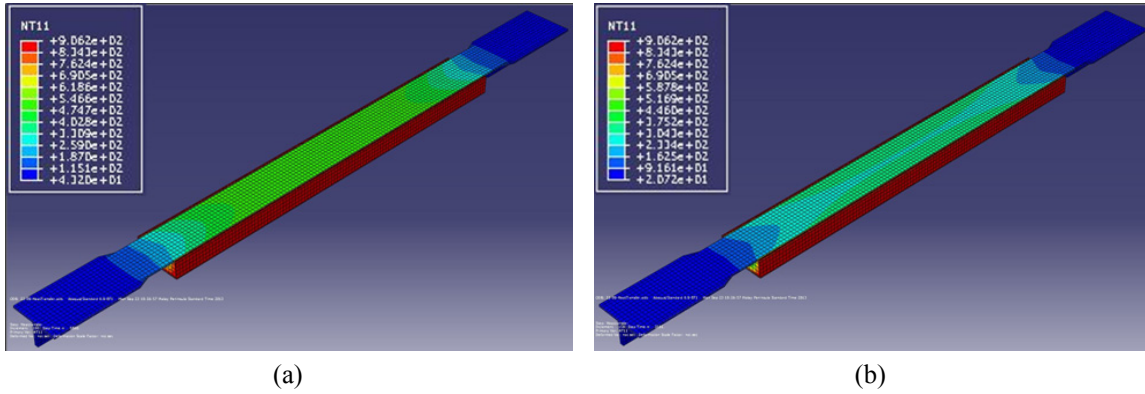


Fig. 10 Temperature distribution across the cross section and along the length of BRB element for (a) sample T1; and (b) sample T2 (units for both legends are in °C)

of the brace (steel tube) to the middle part (steel core) in sample T1 was carried out more rapidly compared to sample T2. This is attributed to the higher conductivity of steel rebar in contrast to the concrete material.

Comparing the temperatures of samples at the time when the heating of standard sample (T1) was terminated, i.e., 43 minutes, it was clear that the maximum temperature for sample T1 was 361°C. For sample T2 it was 314°C, where it was 47°C lower than that of T1. Based on that, it can be concluded that by changing the gap filler material from metal to concrete, it behaves as a refractory coating for the steel core and enhances the efficiency of steel core in resisting the fire loading.

4.3 Effect of the size of the gap at the steel core-restrainer interface

With the purpose of investigating the influence of the existed gap's size (at steel core-restrainer interface) on the fire resistance of the core in BRBs, the gap thickness was made thicker than the

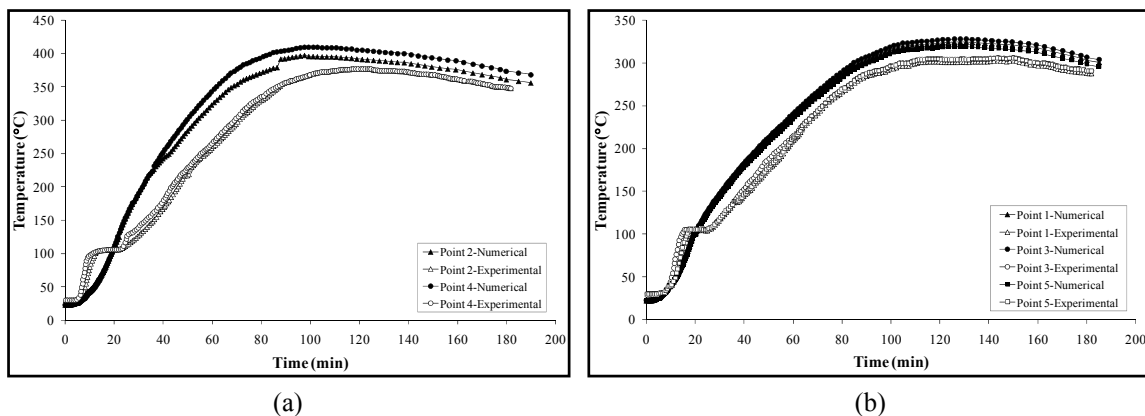


Fig. 11 Comparison of $T-t$ curves for BRB core section at (a) points 2 and 4 and (b) points 1, 3 and 5 in sample T3

standard sample for sample T3 as readily described in Fig. 2. Temperature-time histories at the specified points of the core in sample T3 were compared with the corresponding curves resulted from the referenced test (Saitoh *et al.* 2005) in Fig. 11.

FE results showed that sample T3 experienced the highest temperature of about 398°C after 112 minutes of heating (Table 2), where a comparative temperature of 371.6°C after 116 minutes was recorded in the test. By comparing the maximum temperatures and the corresponding times for T3 and the standard sample, it can be observed that specimen T3 was able to tolerate about 31 minutes more heating time, with lesser maximum temperature of about 47°C than T1 (Table 2).

On the other hand, comparison of samples T2 and T3 revealed that the heating time for sample T3 was about 3 minutes more than T2 and the maximum temperature of the core in T3 was about 42°C less than T2. Hence, it can be concluded that if the dimension of the gap became larger (with the same filler material), the heating time to reach a certain temperature would be longer. Meanwhile, comparing the temperatures at 48 minutes, which was the time when the heating of T2 was stopped, temperatures for T2 and T3 was 320°C and 244°C, respectively (Table 2). T3 showed a lower temperature with a difference of 76°C. Consequently, by enlarging the size of the filler and increasing the gap thickness, the efficacy of the gap to behave as a refractory coating for the steel core in BRBs could be improved under fire condition. This concept is apparent also by comparing the temperatures of all samples at 51 minutes, which was the time when the heating of T3 was discontinued. Sample T3 had the least temperature of 253°C while those of T2 and T1 were 327°C and 371°C, respectively.

Although altering the type of gap filler material and changing the size of gap at the steel core-concrete interface affected the fire resistance of the core in BRBs, none of the specimens could stand the proposed 1 hour of heating time. This observation was concluded from both the FE simulation and the referenced experimental work. Also, it is worthwhile to notice that the entire bracing elements buckled under fire condition (Fig. 12). This occurred due to the decrement of binding force in the BRB restraining system at elevated temperatures.

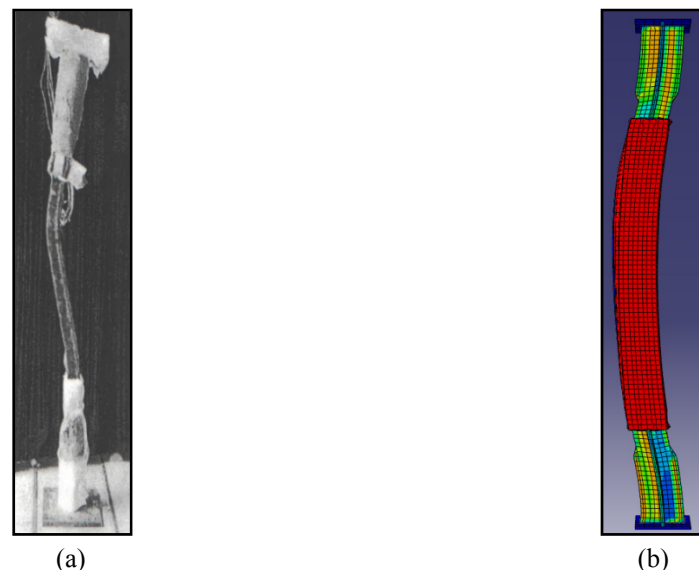


Fig. 12 Buckled shape of specimen after heating, observed for sample T2 (as an example) from (a) experimental test (Saitoh *et al.* 2005); and (b) numerical model

It is worth mentioning here that although the entire BRB samples buckled at elevated temperatures (they buckle at higher temperatures compared to the conventional types), still better efficiency of BRB system in resisting fire in comparison to the ordinary bracing system has been investigated thoroughly by the authors in reference (Talebi *et al.* 2014b). Besides, Saitoh *et al.* (2005) had shown that the tolerable heating time could be enhanced considerably with much lower temperatures recorded in the steel core by using the fireproof coatings on the exterior surface of the restrainer in BRBs. Moreover, since the fire insulation coatings enable the steel casing to avoid direct contact with the fire compartment, the maximum temperature experienced by the restrainer would be much lesser than in the standard case. Consequently, the binding force was almost as effective as in normal temperature in preventing the overall buckling of BRB element at fire.

4.4 Effect of the size and type of gap-filler material on axial contraction of BRB element

As mentioned in Section 3.5, the selected specimens were free to move in the axial direction at the top support. Thus, owing to the applied axial force and a large generated compressive stress (due to temperature rise) in a heated element, its top location descended downwards. Consequently, the axial contractions were experienced by BRB heated elements. Numerical results showed that the variation in the gap size and the type of its filler material had the effect not only on the fire resistance of BRBs' principal part, i.e., steel core, but also considerably on the axial contraction level of the specimens (Fig. 13).

The contraction level increased corresponding to a greater thermally induced force. This phenomenon shown in Fig. 13, which reveals that, the greatest contraction was experienced by sample T1 with a value of 114 mm (point A). The comparative level was 104.4 mm in the referenced test. In essence, steel rebars in neighbouring of the core in specimen T1 behaved as a thermal bridge for temperature distribution from the restrainer to the core, owing to high conductivity of steel material (Saitoh *et al.* 2005). That led to a dramatic increase in core's temperature, followed by experiencing a higher level of axial contraction (point A in Fig. 13). By the replacement of concrete material instead of steel rebar in samples T2 and T3, the axial contraction levels had been significantly reduced to 47.5 mm and 45.8 mm, respectively (points B and C in Fig. 13, respectively). The corresponding values from the test were 36.4 mm and 35 mm, respectively.

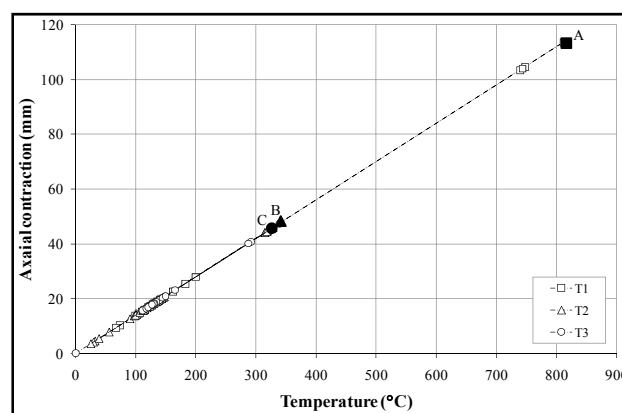


Fig. 13 Comparison of axial contraction levels experienced by three samples

4.5 Effect of the cross-sectional shape of bracing element on fire resistance of BRBs

The numerical heat transfer analyses showed that for a rectangular cross-sectional BRB, four corners of the steel tube casing were expected to have higher temperatures than the regions faces as shown in Fig. 5(a). It was envisaged that the heat input for the rectangular cross section type occurred from two directions onto the heated surfaces. Hence, the temperatures in the corners of adjacent surfaces increased rapidly. This observation was similar to the formerly known tests (Saitoh *et al.* 2005). If the cross-sectional shape of the bracing element was circular (with the same section area), the heat input was exerted in a singular direction uniformly on all external surfaces (Fig. 14) such that the fire-resistant behaviour of BRBs was enhanced compared to that with equivalent rectangular cross sections.

5. Conclusions

Numerical models consisted of two sequentially-coupled analysis steps, namely, heat transfer and stress were utilized to represent the behaviour of BRBs when exposed to standard fire loading. Results from the proposed FE models were verified and they conformed well to those of the tests reported by Saitoh *et al.* 2005. The following conclusions were drawn from the current study:

- The numerical thermal results reflected the temperature change of component section clearly and intuitively:
 - The temperature gradient reduced gradually along the normal direction of steel tube surface exposed to fire.
 - The external surface had the highest temperature (almost near to the fire compartment temperature) and the temperature gradient of the far section, i.e., the restrained segment of the steel core, showed the least.
- The fire resistance of the core could be improved impressively by altering the filler material in the existed gap (at the steel core-restrainer interface) from steel to concrete.
- Enlarging the size of gap and increasing the thickness of in-filled material provided better performance such that the gap acted as a refractory coating for the steel core, resulting in enhanced fire resistance of the core.
- The main influence of altering the type of gap-filler material on the performance of BRBs at fire was manifested in the form of contraction level of element due to thermal loading.
- By enlarging the gap size as well as changing its filler material from steel to concrete, the contraction level of BRB element was reduced dramatically due to greater reduction in the maximum temperature experienced by the core. However, the size factor was not as effective as altering the material from metal to concrete.
- The use of a circular cross-section BRB replacing that of rectangular altered the heat input direction from two to only one, so that the fire-resistant performance of BRBs could be improved.
- The studied BRB samples buckled under fire condition, due to the reduction in binding force in BRB restraining system, at higher elevated temperatures in comparison to the conventional types.
- Using a refractory coating at the exterior surface of the restrainer, the tolerable time of heating could be enhanced in BRBs by preventing the brace from overall buckling due to fire.

Acknowledgments

The research work benefitted from the supports provided by the School of Graduate Studies (SPS), Universiti Teknologi Malaysia (UTM).

References

- ABAQUS (2008), ABAQUS analysis user's manual; SIMULIA, Providence, RI, USA.
- Asgarian, B. and Shokrgozar, H.R. (2009), "BRBF response modification factor", *J. Construct. Steel Res.*, **65**(2), 290-298.
- Clark, P., Aiken, I., Kasai, K., Ko, E. and Kimura, I. (1999), "Design procedures for buildings incorporating hysteretic damping devices", *Proceeding of 69th Annual Convention, SEAOC*, Sacramento, CA, USA, October.
- Espinos, A., Gardner, L., Romero, M.L. and Hospitaler, A. (2011), "Fire behaviour of concrete filled elliptical steel columns", *J. Thin-Wall. Struct.*, **49**(2), 239-255.
- Eurocode 3 (EC3) (2005), Design of steel structures-part 1-2: general rules -structural fire design, British Standards Institution, BS EN 1993-1-2, London, UK.
- Eurocode 4 (EC4) (2005), Design of composite steel and concrete structures- part 1-2: general rules- structural fire design, British Standards Institution, BS EN 1994-1-2, London, UK.
- Ho, C.T.T. (2010), "Analysis of thermally induced forces in steel columns subjected to fire", Masters Thesis; Submitted to the University of Texas at Austin, TX, USA.
- Hong, S. and Varma, A.H. (2009), "Analytical modeling of the standard fire behavior of loaded CFT columns", *J. Construct. Steel Res.*, **65**, 54-69.
- International Code Council (ICC) (2009), International Building Code; Falls Church, VA, USA.
- ISO (International Standards Organization) (1980), ISO 834: fire resistance tests, elements of building construction, Switzerland.
- Jankowiak, T. (2005), "Identification of parameters of concrete damage plasticity constitutive model", Poznan University of Technology, Poznan, Poland, ISSN 1642-9303.
- Korzekwa, A. and Tremblay, R. (2009), *Numerical Simulation of the Cyclic Inelastic Behaviour of Buckling Restrained Braces*, Taylor & Francis Group, London, UK, pp. 653-658.
- López-Almansa, F., Castro-Medina, J.C. and Oller, S. (2012), "A numerical model of the structural behavior of buckling-restrained braces", *J. Eng. Struct.*, **41**, 108-117.
- Lu, H. (2011), "FE modelling and fire resistance design of concrete filled double skin tubular columns", *J. Construct. Steel Res.*, **67**(11), 1733-1748.
- Mirtaheeri, M., Gheidi, A., Zandi, A.P., Alanjari, P. and Rahmani-Samani, H. (2011), "Experimental optimization studies on steel core lengths in buckling restrained braces", *J. Construct. Steel Res.*, **67**(8), 1244-1253.
- Nguyena, A.H., Chintanapakdee, C. and Hayashikawab, T. (2010), "Assessment of current nonlinear static procedures for seismic evaluation of BRBF buildings", *J. Construct. Steel Res.*, **66**(8-9), 1118-1127.
- Sahoo, D.R. and Chao, S.H. (2010), "Performance-based plastic design method for buckling restrained braced frames", *J. Eng. Struct.*, **32**(9), 2950-2958.
- Saitoh, K., Nakata, Y., Murai, M. and Iwata, M. (2005), "Fire-resistant performance of buckling restrained braces using mortar planks", *AIJ J. Technol.*, **22**, 223-226. [In Japanese]
- Sun, R.R., Huang, Z. and Burgess, I.W. (2012), "The collapse behaviour of braced steel frames exposed to fire", *J. Construct. Steel Res.*, **72**, 130-142.
- Takeuchi, T., Hajjar, J.F., Matsui, R., Nishimoto, K. and Aiken, I.D. (2010), "Local buckling restraint condition for core plates in buckling restrained braces", *J. Construct. Steel Res.*, **66**(2), 139-149.
- Talebi, E., Tahir, M., Zahmatkesh, F., Yasreen, A. and Mirza, J. (2014a), "Thermal behaviour of cylindrical buckling restrained braces at elevated temperatures", *The Sci. World J.*, **2014**, 13 p.

- Talebi, E., Tahir, M., Zahmatkesh, F. and Kueh, A. (2014b), "Comparative study on the behaviour of buckling restrained braced frames at fire", *J. Construct. Steel Res.*, **102**, 1-12.
- Zahmatkesh, F. and Talebi, E. (2010), "The performance of bolted slant endplate connections subjected to temperature increase", *Proceedings of the ASME 10th Biennial Conference on Engineering Systems Design and Analysis, ESDA2010*, Istanbul, Turkey, July, pp. 1-11.
- Zahmatkesh, F., Osman, H. and Talebi, E. (2014), "Thermal behaviour of beams with slant end-plate connection subjected to nonsymmetric gravity load", *The Sci. World J.*, **2014**, 13 p.